Journal of the European Ceramic Society 41 (2021) 7543–7551

Contents lists available at ScienceDirect

Journal of the European Ceramic Society

journal homepage: www.elsevier.com/locate/jeurceramsoc

Densification of surface-modified silicon carbide powder by spark-plasma-sintering

Alejandro Montón [a,*], Francis Maury [a], Geoffroy Chevallier [b], Claude Estournès [b], Marc Ferrato [c], David Grossin [a]

[a] CIRIMAT, Université de Toulouse, CNRS, INP- ENSIACET, 4 Allée Émile Monso, Toulouse Cedex 4, 31432, France
[b] CIRIMAT, Université de Toulouse, CNRS, Université Toulouse 3 - Paul Sabatier, 118 Route de Narbonne, 31062, Toulouse cedex 9, France
[c] Mersen Boostec, Zone Industrielle Bazet ouest, 65460, Bazet, France

ARTICLE INFO

Keywords:
Silicon carbide
SiC powder
Spark plasma sintering SPS
Surface modification
Molecular grafting

ABSTRACT

SiC was densified by spark plasma sintering (SPS) and the effects of surface modification of the powder particles on its sintering behavior were investigated. The pressure and temperature conditions were set to 50 MPa and 2200 °C, respectively. Specific SPS experiments at a lower temperature (*i.e.* 1600 °C) was performed to analyze the efficiency of the sintering and the early stage of the densification in softer conditions. The surface functionalization was carried out by grafting a thin molecular layer of a preceramic precursor on the grain surface of SiC particles, which acts as a sintering additive without producing contamination by heteroatoms since, in addition to hydrogen, it contained only Si and C in the same ratio 1:1 as silicon carbide. One of the advantages of this surface functionalization is that it reduces the temperature at which the sintering process begins and therefore it facilitates and increases the densification of the final SiC parts.

1. Introduction

Because of its excellent properties such as its high mechanical stiffness, low density, wide bandgap, low coefficient of expansion, high thermal stability, and resistance to corrosive environments, silicon carbide (SiC) is an advanced ceramic material for many technological applications [1]. Among these applications are high-power microwave devices for commercial and military systems; electronic devices (LED's, MOSFET's); high temperature electronics/optics for automotive, laser processes mirrors and well-logging; rugged MEMSs (micro--electro-mechanical sensors) devices for hostile environments; gas and chemical sensors for internal combustion engines, furnaces and boilers; solar-blind UV photodetectors [2], very high temperature solar absorber [3] and aerospace applications as space telescope mirrors [4] and more generally very large telescopes [5,6].

The manufacture of monoliths SiC parts is very difficult because it is a covalent ceramic which decomposes above 2545 °C to form liquid silicon and carbon [7]. Consequently, under normal conditions, it has no liquid phase. The main difficulty to fabricate massive and dense SiC parts lie in the sintering stage. For example, without any additives, the theoretical density could only be achieved at 2500 °C by a classical hot-pressing process under a pressure of 50 MPa [8]. A number of aids are then used to promote SiC densification, but certain glassy-like phases formed at grain boundaries from heteroatoms may be detrimental to the desired performance and, consequently, mechanical properties can be lowered.

Spark Plasma Sintering (SPS) is an advanced process that was also used to consolidate silicon carbide powder without additives. The first step is to choose the most suitable SiC powder and the second one is to optimize SPS experimental conditions. The SPS process allows various types of materials to be sintered [9] with control microstructure [10] and shape [11]. It relies on pulsed DC current passing through an electrically conducting pressure die containing the sample. Uniaxial pressure is applied during sintering. The main benefit is that full density can be reached fairly easily, the whole experience taking only a few minutes. Unfortunately, like so many other covalent refractory ceramics, even by SPS SiC is very difficult to sinter to a high density without using binder additives (that generally bring heteroatoms that are left in the part) and/or very high pressures.

Thus, to reach high density sintered SiC functional additives are used. In previous studies, it was shown that these aids could lower the sintering temperature. Several compounds were tested as sintering

* Corresponding author.
E-mail address: alejandro.montonzarazaga@ensiacet.fr (A. Montón).

https://doi.org/10.1016/j.jeurceramsoc.2021.07.036
Received 12 March 2021; Received in revised form 14 June 2021; Accepted 18 July 2021
Available online 31 July 2021

Table 1
Summary of the process conditions and main features of PCS and PCS + SiC starting materials sintered by SPS.

Ref.	Year	Powder feedstock	PCS	SPS parameters[a]	Relative density of final parts
Bernardo et al. [18]	2014	PCS + Boron (5% and 10 % wt)	Nipusi® type S, Nippon CarbonCo., Ltd. Mw = 1400	T: 2050 °C R: 100 °C/min P: 16 MPa (T<2050 °), 50 MPa (T = 2050 °) t : 10 min	94 %
Lodhe et al. [21]	2016	PCS after pyrolysis at 1400 °C + SiC whiskers (10−20% vol.)	–	T: 1600−1800 °C R: 100 °C/min P: 50 MPa t : 10 min	95 %
Y. Lee et al. [22]	2018	PCS after pyolysis at 1000 °C	Mw = 13600, ToBeM Tech. Co.	T: 1700−1900 °C R: 100 °C/min P: 40 MPa (T< 2050 °), 80 MPa (T = 2050 °) t : 10 min.	95 %
This work	2021	SiC powder + w/PSE and w/o	PSE: Mw ≈ 250 Starfire® System	T : 600−2200 °C R : 100 °C/min P : 50 MPa (T = 2200 °C) t : 1 min	91−96%

[a]) Temperature (T); Heating Rate (R); Total Pressure (P); Duration in steady state (t).

additives for SiC powder both to enhance the densification rate and to slow down grain growth kinetic. To achieve high densities through solid-state sintering and to avoid the appearance of low corrosion resistance intergranular phases, consolidation of SiC with boron and carbon as sintering additives seems to be the most efficient way [12]. Therefore, boron carbide was found to enhance the hot-pressing behavior of SiC that could be so obtained in a fully dense state [13,14]. These additives permit to reach high density slightly over 2000 °C by means of the reduction of the surface energy of the grains (surfactant effect due to boron) and reaction with residual silica (carbon reduction). Following these results, Maître et al. used SPS method and boron additive to produce fully dense SiC-based materials with several non-oxide secondary phases such as boron carbide (B_4C) or free boron (B) plus free carbon (C) [15]. However, for some applications these additives are considered as contaminants for final parts and as a consequence not acceptable.

For this reason, no additive was used and a stringent optimization of the process parameter was a preferred route. For instance, Guillard et al. applied a specific SPS procedure for synthesizing and densifying pure commercially available submicrometer-sized SiC powder. Using this procedure, a 92 % Relative Density (RD) was achieved. The aim of this previous study was to assess the evolution of SiC grain size and density versus temperature, holding time and pressure on a commercial powder [16]. As another example of pure SiC SPS, Hayun et al. obtained a density of SiC bodies of 3.1870 g/cm^3 (RD = 99 %) in the absence of sintering additives. They have used an SPS treatment at 2050 °C for 10 min, a heating rate of 400 °C/min and a high applied pressure of 69 MPa to densify alpha-SiC powder [17]. However, even with the advantages of SPS, sintering aids are generally required to obtain a dense SiC body.

A potential possibility recently proposed by authors to obtain full-dense SiC body by SPS is the direct use of polymer-derived ceramics as single-source materials, *i.e.* without SiC powder [18]. These pre-ceramic molecular precursors present distinctive features such as low process temperatures and, above all, the possibility of applying forming techniques for conventional polymer processing. However, heating of preceramic polymers generally leads to the formation of cracks and pores in the ceramic products due to gas release and shrinkage resulting from polymerization and crosslinking. Crack free products can be manufactured in the case of fibers, microcellular foams and thin films thanks to the key role of the many interfaces. In these configurations, the material can tolerate both the release of a great amount of gases as by-products (mainly hydrogen and lightweight hydrocarbons) during the polymer-to-ceramic conversion and also the significant volumetric shrinkage up to 60 % [19].

Bernardo et al. analyzed the SPS processability of SiC derived from one of the commercial family of polycarbosilane (PCS) powders (Nipusi® type S, Nippon CarbonCo.,Ltd) featuring a molecular weight (Mw) of 1400 mixed with boron as additive [18]. PCS compounds are inorganic polymer composed of a Si-C backbone leading to a fixed Si/C atomic ratio (characteristic of each PCS compound) and a small amount of hydrogen. Furthermore, they exhibit similar properties as organic polymers, *i.e.* they are meltable, soluble, and unstable at high temperatures. For conversion to silicon carbide, PCS must undergo several steps during heat treatment: formation of oligomers by pyrolysis, usually by dehydrogenation, then polymeric intermediaries, crosslinking, amorphous preceramics, crystallization, and crystal growth. When comparing PCS compounds and SiC powder as starting materials in the sintering process, there are notable differences. In the sintering process for a ceramic material as SiC, a crystallized powder is generally used, whereas PCS is used in an amorphous state after pyrolysis with a Si- or C-rich content depending on its initial composition. Therefore, starting with PCS, several steps must accompany sintering as the events above cited as well as nucleation, crystal growth, and grain growth [20].

More authors explored the use of PCS for densification of SiC by SPS (Table 1). Lodhe et al. studied the phase transition of SiC during SPS, where a PCS was used after pyrolysis at 1400 °C combined with SiC whiskers (10−20% vol.) [21], and Lee et al. sintered PCS (Mw 13600, ToBeM Tech. Co.) powder after pyrolysis at 1000 °C by SPS [22].

The aim of our study is to extend and to explore the use of original PCS compounds as a sintering aid by direct surface grafting on SiC powder. For that, we used a simple and volatile commercially available PCS precursor not yet tested as additive in an SPS process.

Consequently, by means of SPS, the original scientific approach of this work resides in the production of innovative SiC powders that enhance the sintering behavior of SiC by surface functionalization of grains consisting of grafting a molecular nanolayer that does not contain heteroatoms and does not induce the formation of secondary phases. The effects of the surface functionalization have been studied and compared to non-modified SiC powder.

2. Experimental

A commercial compound of the PCS family, namely poly(silaethylene) (PSE) was supplied from Starfire® System (supplier name CVD-4000). It was used for the surface functionalization of silicon carbide powder as SiC forming oligomer and known to lead to the growth of stoichiometric silicon carbide coatings (ratio Si:C = 1:1) without the need for additional reactants by chemical vapor deposition [18]. Its formula is [−SiH2−CH2−]n, n = 3–8), which reveals Si—C covalent bonds already formed and an atomic Si:C ratio = 1:1 as in crystallized silicon carbide. It is a volatile liquid compound, easy to handle and readily available. It produces amorphous hydrogenated silicon carbide coatings by pyrolysis at 800 °C in a chemical vapor deposition process [23].

The SiC samples were spark plasma sintered using a Dr. Sinter 2080 unit, SPS Syntex Inc., (Japan,) available at the Plateforme Nationale

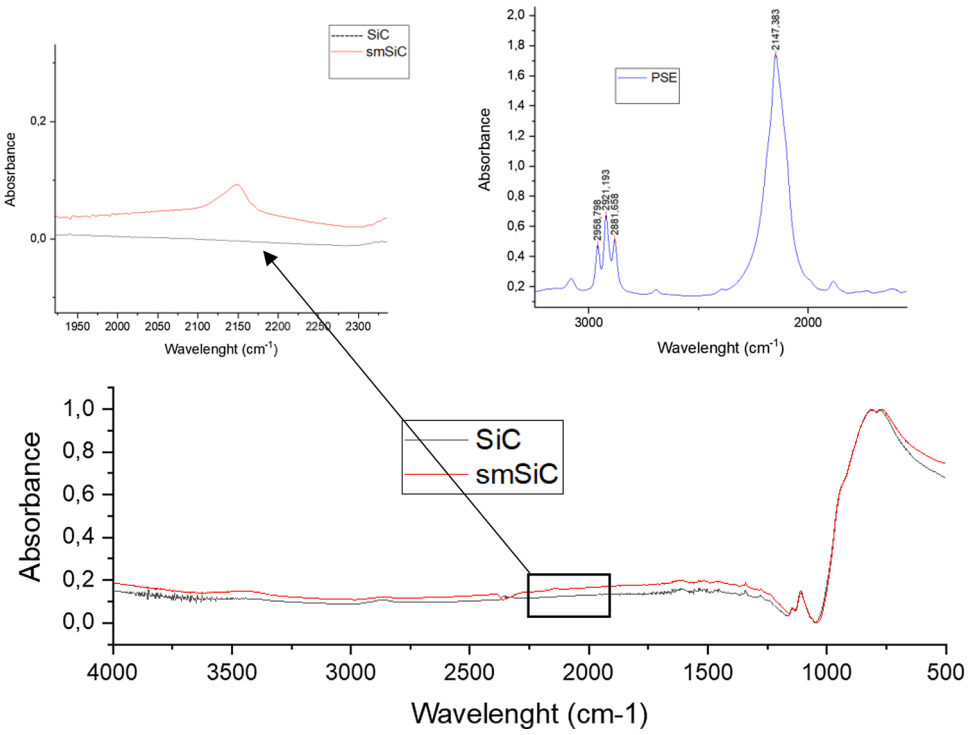

Fig. 1. PSE (CVD-4000), SiC powder and smSiC powder IR spectra.

CNRS de Frittage Flash located at the Université Toulouse 3 Pau l Sabatier (France). The SiC powder was loaded into graphite dies with an inside diameter of 8 mm to produce pellets at least 10 mm thick. Prior this step, a graphite foil (PERMA-FOIL®Toyo Tanso) was systematically placed to cover the inside wall of the die, as well as at the interfaces between the punches/sample and spacers/electrodes. The outside wall of the die was systematically covered with a graphite felt to minimize the heat loss during the experiment. A heating rate of 300 °C/min was used from room temperature to 600 °C, where a 1-min dwell was applied. Then, a heating rate of 100 °C/min between 600 and 2200 °C was applied. An optical pyrometer (IR-AH series Chino), focused inside a little hole (1.8 mm in diameter and 3 mm in depth) located in the outside wall of the die was used to control and monitor the temperature. For one pure SiC powder and a surface-modified Silicon Carbide powder (namely smSiC) the heat treatment was stopped at 1600 °C to observe and compare the early stages of sintering. Pressure was set at 50 MPa at room temperature and maintained up to the end of the dwell. In each case, pressure was released at the end of the holding time and the cooling rate down to 1000 °C was around 400 °C/min. Some graphite paper, used for the die protection, remaining at the surface of the pellets after the SPS step was removed by soft polishing of the samples using abrasive paper. Then, density of the final specimens was determined according to Archimedes' principle and compared to SiC theoretical density [1].

The structure of the samples was analyzed using Cu K-alpha radiation (λ = 1.5406 Å) over the 2θ range of 20–80°using X-ray powder diffraction (Diffractometer D8−2) and the phase composition was determined by the Rietveld method from XRD patterns with MAUD, following the strategy developed by Hongchao et al. [24]. Their microstructure was studied using Scanning Electron Microscopy (LEO435VP) The samples for the microstructural characterization were prepared using a standard metallographic procedure. The samples were polished with diamond paste and subsequently introduced in hard resin to study the cross section of the material. The cut was made with a cutting machine (Mecatome T210) using a diamond blade. FT-IR spectra of the PSE (CVD-4000), SiC powder and smSiC powder were obtained over the range of 4000 to 400 cm − 1 using a Nicolet 5700 spectrometer. KBr discs were used, prepared by compressing a finely ground mixture of about 3 mg of the sample and 300 mg of KBr powder. Raman micro-spectroscopy using a Labram HR 800 Yvon Jobin Raman confocal spectrometer with a confocal hole of 100 mm and an argon laser emitting at 532 nm provided chemical and structural characterizations of the samples. We have recorded the Raman spectra by scanning the entire range of interest 550–1050 cm − 1. References to standard transform acoustic phonons (TA), transverse optical phonons (TO) and longitudinal optical phonons (LO) were obtained from literature for the following basic polytypes: α-SiC (6H-SiC) and 4H-SiC — both have hexagonal symmetry and wurtzite structure, and 15R-SiC [25,26].

3. Results and discussion

PSE has been grafted onto the surface of SiC particles in the form of a conformal coverage molecular layer, which avoid the excess of oligomer that can be provided by the feed powder.

Alpha-SiC, powder with a mean grain size of 2 μm provided by Mersen Boostec were used in this project. As it was already mentioned by E. Lidén [27] et al. and experimentally proofed by Luo et al. [28], it is important not to use an excess of polymer that can be grafted onto the surface of the powder, since this could increase the specific surface area, change the morphology of the powder too much and the coupling agent could hardly infiltrate into the nanoparticle agglomerates of the powder and reduce the graft efficiency. Therefore, it was first necessary to calculate the amount of oligomer required for a conformal coverage of the powder grains with a molecular monolayer of PSE. The powder grains were supposed monodisperse and spherical with an average diameter of 2 μm. An approximate value of ∼ 1 *wt*.% of PSE was found. Then the surface-modified silicon carbide (smSiC) powder was prepared by a wet route. A suspension of the alpha-SiC powder was stirred in toluene in a Schlenk tube, then a PSE solution (∼ 1 *wt*.%) in toluene as a solvent was added dropwise under argon atmosphere using a vacuum manifold to avoid premature degradation of this PCS compound. This suspension was magnetically stirred for 1 h at 60 °C, and then it was transferred into a rotative evaporator for 3 h at 60 °C to remove slowly the solvent and the PSE excess. At the end, the smSiC powder was stored

Table 2
Experimental and relative density for SPS-SiC and SPS-smSiC. The relative intensity was determined compared to the theoretical value of alpha-SiC. The temperature and pressure experimental conditions were set constant at 50 MPa and 2200 °C with a rate of 100 °C/min for all the samples. The steady state temperature was maintained constant for 1 min.

Sample name	Sintering Temperature (°C)	Powder feedstock	Experimental density (g/cm^3)	Relative density (%) (theo = 3.217 g/cm^3)
SPS-SiC-1	2200	SiC	2.921	91 %
SPS-SiC-2	2200	SiC	2.933	91 %
SPS-SiC-3	2200	SiC	2.934	91 %
SPS-SiC-1−2-3*	2200	SiC	**2.929 ±0.007**	91 %
SPS-smSiC-1	2200	SiC + PCS (1 wt%)	3.046	95 %
SPS-smSiC-2	2200	SiC + PCS (1 wt%)	3.097	96 %
SPS-smSiC-3	2200	SiC + PCS (1 wt%)	3.005	93%
SPS-smSiC-1−2-3*	2200	SiC + PCS (1 wt%)	**3.048 ± 0.046**	95 %
SPS-SiC	1600	SiC	2.472	61 %
SPS-smSiC	1600	SiC + PCS (1 wt%)	2.780	72 %

* Average values of data above.

in the dry atmosphere of a vessel before its use in SPS.

Indeed, this strategy does not change significantly the main features of the SiC powder as the specific surface area and the morphology. Furthermore, this coupling agent infiltrates into the particle aggregates and increases the grafting efficiency [27]. This original approach is highlighted in the Table 1 summarizing a brief state-of-the-art of SPS sintering of SiC using PCS compounds.

The liquid oligomer samples were examined as a thin film between KBr plates. Fig. 1 shows the FT-IR spectra. The bands are assigned with reference to literature on known organic compounds and polycarbosilane (PCS) [29,30]. In the spectra, we observe the CH stretching region (3100−2800 cm^{-1}) and the strong band at 2150 cm^{-1} assigned to the SiH. Regarding smSiC powder IR spectra, SiH band is detected due to the oligomer grafting onto the SiC particles. Consequently, SiC powder IR spectra doesn't show this band.

3.1. Relative density

Table 2 summarizes the processing conditions applied to the investigated SiC-based ceramics, along with measured density. Interestingly, a high reproducibility was obtained using the as-received untreated SiC powder with a relative density of 91 % for several runs of only 1 min. For the functionalized SPS-smSiC samples the relative density in the same conditions reaches the narrow range 93–96 %, which also confirms a very good reproducibility. If this very low dispersion is considered significant, it can then be assumed that it would reflect some differences in the grafting efficiency of the different batches of smSiC powders.

Density of these various pellets shows differences versus the various powders used as starting materials. In general, SPS-smSiC samples prepared at 2200 °C for only 1 min exhibit the highest relative density (95 ± 1%). Their relative density is approximately 4% higher than that of SiC samples prepared using ungrafted powders (Table 2). Thus the density achieved is as high as those obtained previously by directly using a pretreated PCS compound and additives (Table 1). We retain that dense SiC bodies were obtained under our SPS conditions for both types of SiC powders used (with and without grafting).

We will further discuss the samples heat treated up to only 1600 °C for 1 min (namely SPS-SiC and SPS-smSiC) in section 4.3 (Sintering initiation). We will see that the differences in density mentioned above are confirmed and even reach 9%.

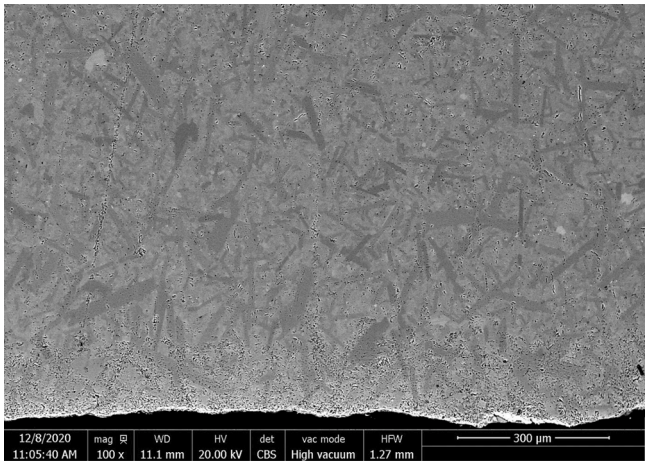

Fig. 2. SEM fracture micrographs of the SPS-SiC-1 sample after polishing (final SPS temperature 2200 °C).

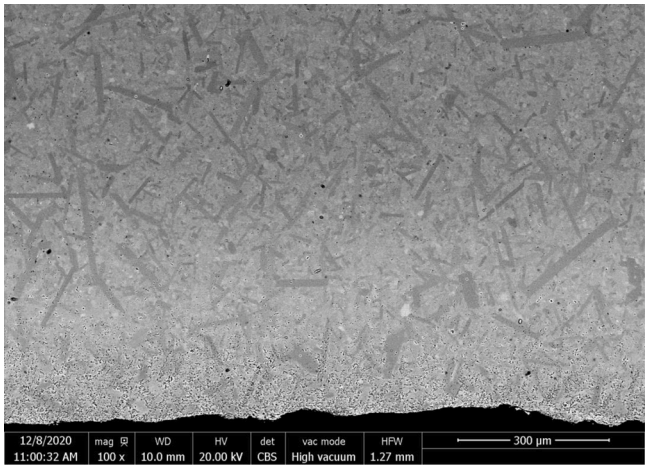

Fig. 3. SEM fracture micrographs of the SPS-smSiC-2 sample after polishing. (final SPS temperature 2200 °C).

3.2. Microstructural and crystallographic characterization

SPS-SiC and SPS-smSiC pellets exhibit similar grain morphologies. Both polished SiC (Fig. 2) and polished smSiC samples (3) show a low porosity which increases at the edges of the pellet of 8 mm in diameter (see for instance at the bottom of micrographs of Figs. 2 and 3). However, no specific changes are found between them. This observation is in accordance to the density measurement since we observe practically full dense SiC and smSiC bodies with RD ≥ 91 % (samples SPS-SiC-1 to SPS-smSiC-2 in Table 1). The SEM images in Figs. 2 and 3 have been recorded using a concentric backscatter detector (CBS) and, usually, the contrast originates both from changes in the composition and topography. However, since the samples have been carefully polished, the different darker/brighter areas shown in the SEM image of Fig. 3 are preferentially due to different crystallographic orientation (or SiC polymorphs) since no chemical modification is detected by an EDS line-scan analysis, as confirmed by the constant value of the normalized Si intensity through a dark area of about 24 µm wide. Also, EDS analysis excludes the formation of elemental Si that would come from the decomposition of SiC. This is in agreement with the fact that such a decomposition is

Table 3
Phase composition determined by Rietveld method [24] of XRD patterns of SiC and smSiC samples prepared by SPS compared to the powders used.

Sample	Name	SiC-6H	SiC-15R	SiC-4H	Rwp (%)	Rexp (%)
SiC powder	As-received	93.02 % ± 1.30	3.35% ± 0.47	3.63% ± 0.51	14.23	3.05
smSiC powder	After grafting	93.24 % ± 1.05	2.08% ± 0.56	4.47% ± 0.66	22.54	4.24
SiC (2200 °C/1 min)	SPS-SiC-1	70.06% ± 0.78	2.06% ± 0.21	27.88% ± 0.39	6.81	3.38
smSiC (2200 °C/1 min)	SPS-smSiC-2	72.60 % ± 0.95	1.68% ± 0.23	25.71% ± 0.38	8.10	3.29
SiC (1600 °C/1 min)	SPS-SiC	93.89 % ± 0.90	3.03% ± 0.18	3.08% ± 0.22	8.29	3.24
smSiC (1600 °C/1 min)	SPS-smSiC	94.42 % ± 0.85	2.61 % ± 0.16	2.97% ± 0.23	7.58	3.31

expected only at 2545 °C [7].

The phase composition of the SiC powder used was investigated by XRD (Figs. 2 and 3) and data are reported in Table 3. It is shown that as-received SiC powder contains only two phases: the hexagonal-wurtzite SiC-6H (also called α-SiC) and the rhombohedral SiC-15R in the proportion 85 % and 15 % respectively. No significant difference was found for the smSiC powder, which was expected since the molecular grafting was a soft wet method that does not require high temperatures.

The XRD analysis of the SiC samples densified by SPS at 2200 °C as SPS-SiC-1 (Fig. 2) exhibits 3 different crystal phases: SiC-6H and SiC-15R like originally in the starting powder plus the hexagonal SiC-4H. The graphite signals at about 2theta = 26.5 and 78 deg are also present on the XRD patterns but they are due to the contamination by the graphite dies and therefore graphite was not considered subsequently. Decomposition of silicon carbide did not occur since elemental silicon is not detected. From the Table 3, it can be seen that the proportion of the new phase SiC-4H is 25 % and it was preferentially produced to the detriment of SiC-15R and for a smaller part from SiC-6H.

The XRD pattern of the smSiC sample also prepared at 2200 °C as SPS-smSiC-2 (Fig. 3) exhibits the same three SiC phases with very close proportions as reported in Table 3. It is notable that the SiC-4H content is only 22 % instead of 25 % using as-received SiC powder. If it is assumed that these differences are significant, this can be attributed to an effect of molecular grafting which would limit the structural transformations.

The XRD patterns of SiC (SPS-SiC) and smSiC (SPS-smSiC) samples prepared at only 1600 °C are shown in Figs. 5 and 6 respectively. Both patterns are similar to that of the as-received SiC powder, *i.e.* no evidence for the presence of SiC-4H was found. This is consistent with the fact that for these low temperature samples the SPS process was interrupted before reaching the sintering SiC temperature and, consequently, no SiC-4H transformation can occur [31,32].

These results show that the use of PSE oligomer as SiC grafting molecular precursor does not change very significantly the final phase composition of the SPS samples and its conversion to SiC is fulfilled.

A RAMAN analysis was realized on the samples SPS-SiC-1 and SPS-smSiC-2 (Fig. 7). In this study, the focus is on the most intense FLO and FTO modes. The presence of three polytypes was identified at the initial state: SiC-4H, -6H and -15R; written in the Ramsdell notation. These polytypes differ by their crystalline lattice and stacking order. The associated Raman spectrum is a combination of these polytypes from which some peaks are characteristics of one polytype. For example, the peak at 789 cm − 1 characterizes the SiC-6H, the peak at 777 cm − 1, the SiC-4H and the peak at 785 cm − 1, the SiC-15R [25,26]. This result is in accordance with the XRD pattern of the SiC and smSiC sample also prepared at 2200 °C as SPS-SiC-1 and SPS-smSiC-2 (Figs. 5 and 6). They exhibit the same three SiC phases with very close proportions as reported.

3.3. Sintering initiation

Figs. 8 and 9 indicate the temporal variation of temperature and displacement during the SPS process. The displacement is not corrected for the contribution of the components of the SPS column, *i.e.* it takes into account the graphite and SiC contribution. For these two experiments, the process was stopped at T = 1600 °C. From the red curve of sample SPS-SiC (Fig. 8), we observe a slight expansion at the beginning of the SPS process that is caused by the thermal expansion of particles and die, as well as gas release [33]. This low temperature expansion occurs in two main steps: the first one up to 100 s and the second up to approximately 300 s to reach a plateau. In this low temperature range, the behavior of the smSiC sample (SPS-smSiC) is close to that of SiC (SPS-SiC) except the plateau is reached after 200 s (Fig. 9) instead of 300 s for the SiC sample (Fig. 8). The great increase of the displacement curve at high temperature occurs faster for the SPS-smSiC sample (Fig. 9) compared to the SiC one (Fig. 8), approximately at 650 s and 750 s respectively. For both samples, the relationship between the temperature and the displacement shows that the displacement starts at 1060 °C in the smSiC sample and at 1240 °C in the SiC sample (Fig. 10). This change in the displacement curve means a dimension shrinkage of the powder [34]. Wherewith it can be deduced that the sintering process begins with a difference between both powders of *ca.*180 °C, revealing that sintering is significantly facilitated using smSiC powder. Then, the temperature and pressure remained constant during the SPS process as

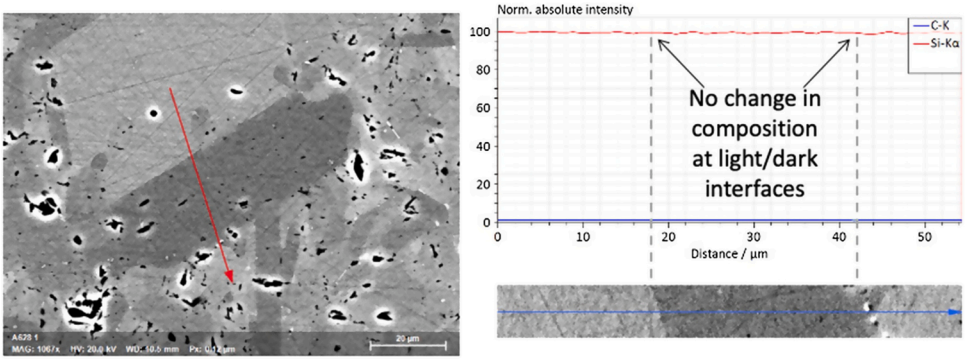

Fig. 4. SEM fracture micrographs of the SPS-smSiC-2 sample after polishing prepared with a final SPS temperature in the steady state of 2200 °C for 1 min (left). EDS line-scan analysis along the red arrow across the dark area showing a constant Si content (right). (For interpretation of the references to colour in the Figure, the reader is referred to the web version of this article).

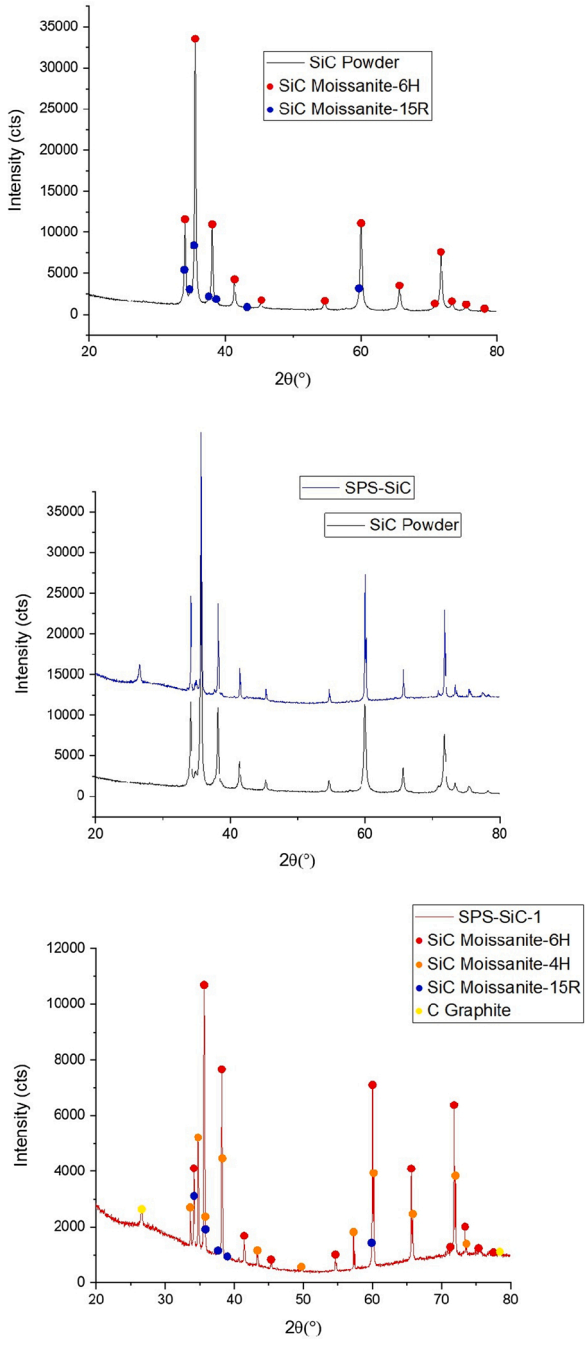

Fig. 5. XRD pattern of SPS-SiC-1, SPS-SiC and SiC powder.

explained in section 3.

Regarding the microstructure, the porosity of the SPS-SiC (Fig. 11) and SPS-smSiC (Fig. 12) samples appear to be both closed and open (as suggested by some extensive ramifications of the porosity network). Anyways, the total porosity of these samples determined using the ImageJ software from SEM images as in Figs. 11 and 12 gave approximate values of 39 % and 32 % for the SiC (SPS-SiC) and smSiC (SPS-smSiC) samples, respectively. This result is in very good agreement with the relative density measured by the Archimedes method since the values of 61 % and 72 % were found (Table 1). Clearly, SEM analysis and density measurements demonstrate that, compare to raw SiC powder, a better densification is obtained with the use of SiC powder previously grafted with the PSE oligomer. This is in good agreement with the sintering initiation difference that we measured *in situ* during the SPS process as reported in Fig. 10.

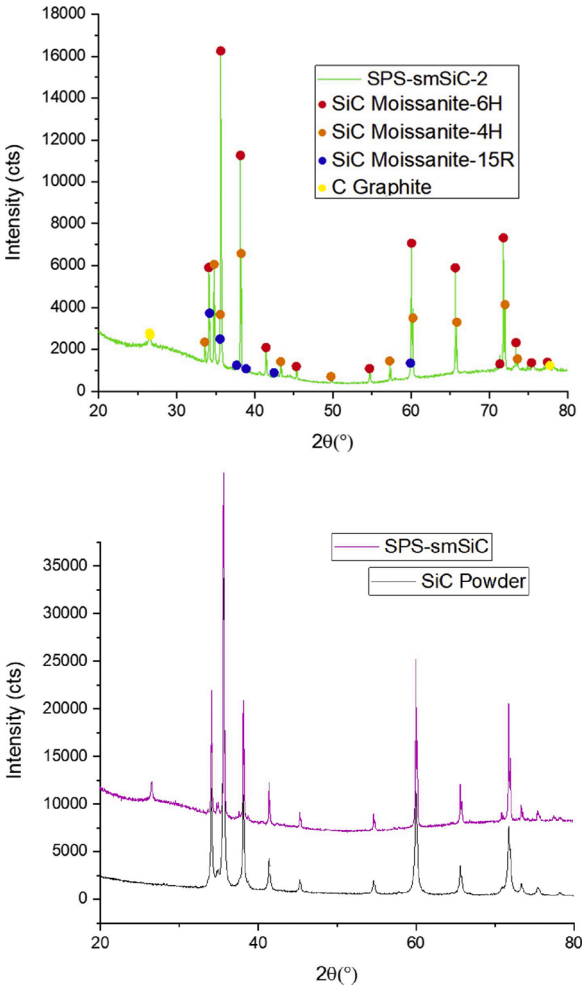

Fig. 6. XRD pattern of SPS-smSiC, SPS-smSiC-2 and smSiC powder.

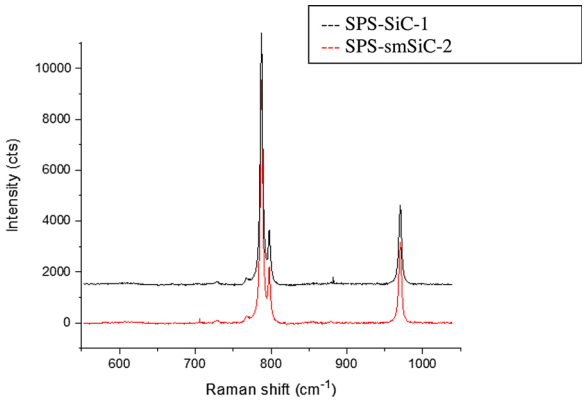

Fig. 7. Raman pattern of SPS-SiC-1 and SPS-smSiC-2.

Despite the relatively large porosity of the SPS samples prepared at 1600 °C (Fig. 11 and Fig. 12), their SEM analysis did not reveal the obvious presence of dark zones unlike the samples densified at 2200 °C (Figs. 2 and 3). We assumed that these bright/dark contrasts were mainly due to differences in crystallographic orientation as no variation in atomic composition was found by EDS (Fig. 4). According to this hypothesis, the dark structures could for example be attributed to the SiC-4H phase which is barely present in the starting powder but which forms during SPS runs at 2200 ° C. The minor presence of this SiC-4H phase in samples prepared at 1600 °C was revealed by XRD analyzes.

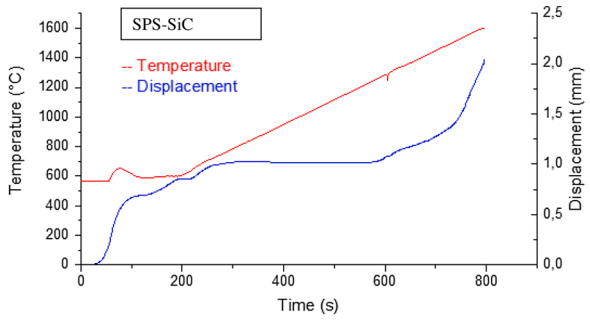

Fig. 8. Temporal temperature and displacement changes during the SPS process of the sample SPS-SiC (final SPS temperature 1600 °C).

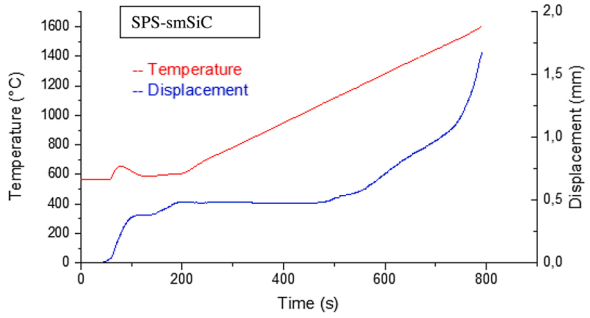

Fig. 9. Temporal temperature and displacement changes during the SPS process of the sample SPS-smSiC (final SPS temperature 1600 °C).

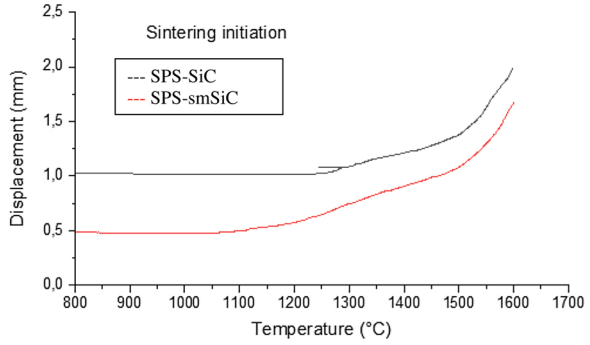

Fig. 10. Sintering initiation: variation of the displacement versus the temperature during the SPS process of the samples SiC (SPS-SiC; black curve) and smSiC (SPS-smSiC; red). Increasing displacement in graphs means dimension shrinkage of the powder compact according to [34]. (For interpretation of the references to colour in the Figure, the reader is referred to the web version of this article).

In addition, the absence of dark areas on the SEM micrographs of these low temperature samples supports our hypothesis to attribute the presence of dark areas to the SiC-4H phase. We then performed image treatment of the micrographs of Figs. 11 and 12 using ImageJ software and we found that the dark areas represented 27 % and 24 %, respectively for the SPS-SiC-1 and SPS-smSiC-2 samples. This is in very good agreement with the proportions of the SiC-4H phase determined by Rietveld analysis [24] of the XRD phases which were respectively 27 % and 22 % (Table 3) and the RAMAN spectra. This good overall consistency gives credibility to our hypothesis, which can be checked later, for example by TEM analyzes.

4. Conclusion

Dense silicon carbide specimens were fabricated by SPS process at

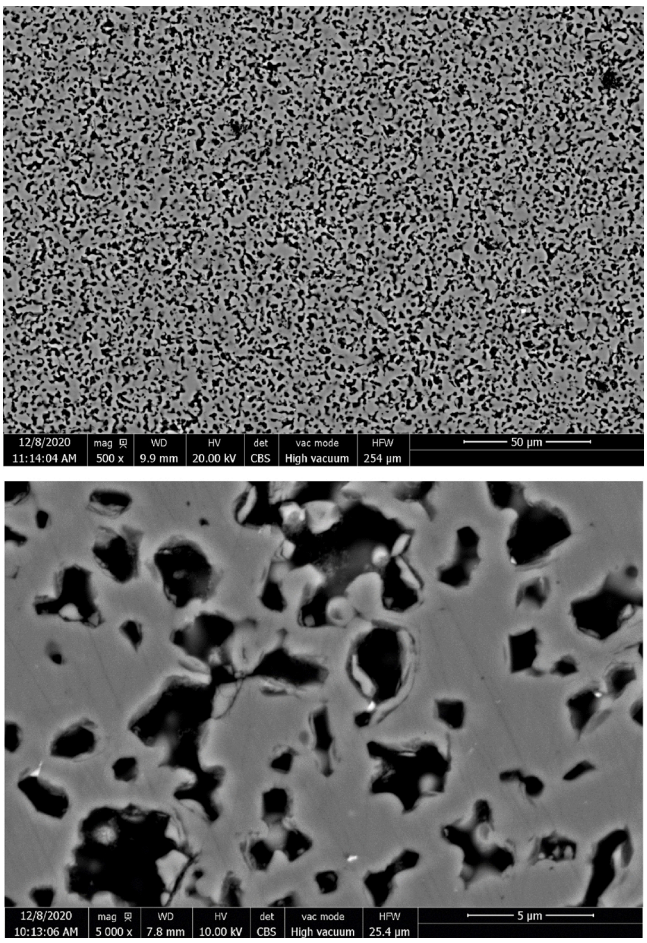

Fig. 11. SEM fracture micrographs of the SPS-SiC sample after polishing. The final temperature was stopped at 1600 °C to avoid a full densification.

2200 °C and 50 MPa for only 1 min in this steady stage. The SiC samples were densified up to 91 % and the surface-modified smSiC sample up to 96 % using the same SPS conditions. The final porosity is very low since it lacks only 4% in density compared to theoretical bulk SiC. Interestingly, the densification is always found better for smSiC than for raw SiC sample. Consequently, the poly(silaethylene) (PSE) grafted onto the SiC grains is completely converted into SiC. This confirms that thanks to its atomic ratio Si:C = 1:1 (as in stoichiometric SiC) and to the absence of heteroatoms, it is a suitable preceramic molecular precursor for SiC. This was previously demonstrated for CVD process for the growth of SiC coatings [23] and this is extended here for the fabrication of 3D SiC parts by SPS technique.

Moreover, the surface-grafting of the oligomer-derived ceramic does not affect the final phases of the dense bodies since they are all composed of the three phases SiC-6H, SiC-4H and SiC-15R. This study allowed us to determine that the surface modification of the SiC powder decreases the sintering start temperature by about 180 °C and therefore a better densification is obtained, which is a good result for developing a more energy efficient SPS process.

Finally, compared with previous results [18,21,22], an innovative method has been used to graft a oligomer used as SiC molecular precursor in a controlled way on the surface of the SiC particles instead of using this preceramic precursor directly after pyrolysis or mixed with heteroatoms as boron additives to obtain a significantly improved final densification. Taking into account progress to understand and simulate SPS processes [35,36], this result is a new step towards the achievement of a 3D SiC part by SPS.

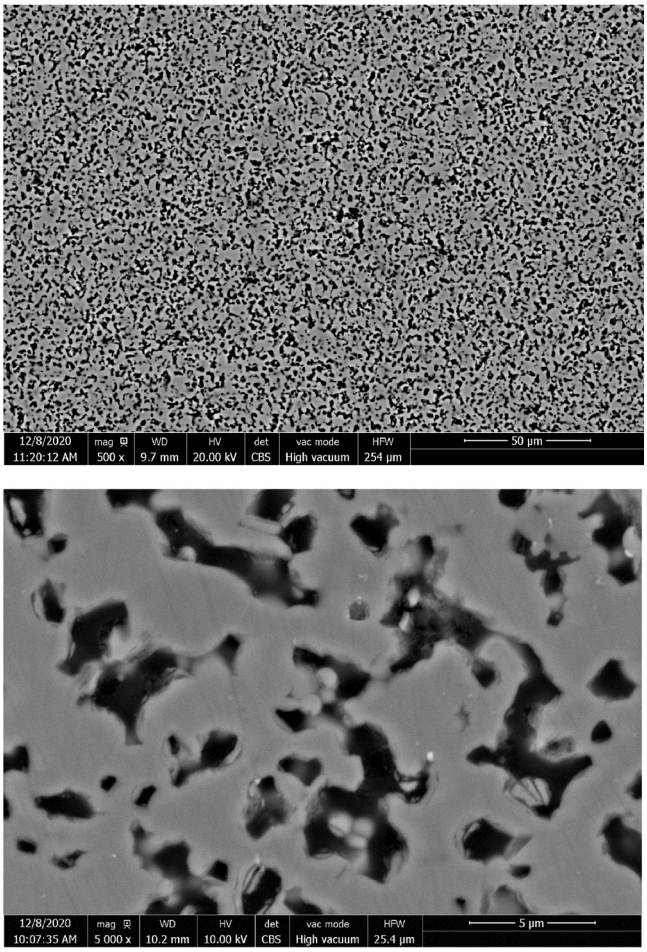

Fig. 12. SEM fracture micrographs of the SPS-smSiC sample after polishing. The final temperature was stopped at 1600 °C to avoid a full densification.

Declaration of Competing Interest

The authors declare that they have no known competing financial interests or personal relationships that could have appeared to influence the work reported in this paper.

Acknowledgements

This project, DOC-3D-Printing, has received funding from the European Union's Framework Program for Research and Innovation Horizon 2020 (2014-2020) under the Marie Skłodowska-Curie Grant Agreement No. [764935].

References

[1] G.L. Harris y, in: Institution of Electrical Engineers (Ed.), Properties of Silicon Carbide, INSPEC, the Inst. of Electrical Engineers, London, 1995.
[2] T. Ohji, M. Singh, M. Halbig (Eds.), Advanced Processing and Manufacturing Technologies for Nanostructured and Multifunctional Materials II: A Collection of Papers Presented at the 39th International Conference on Advanced Ceramics and Composites, John Wiley & Sons, Inc., Hoboken, NJ, USA, 2015, https://doi.org/10.1002/9781119211662.
[3] C. Leray, et al., «Design and Proof of Concept of an Innovative Very High Temperature Ceramic Solar Absorber», Abu Dhabi, United Arab Emirates, 2017, p. 030032, https://doi.org/10.1063/1.4984375.
[4] M. Bougoin, C. Coatantiec, J. Lavenac, V. Costes, «A new technological step for sic mirrors preparing OTOS», in: International Conference on Space Optics — ICSO 2014, Tenerife, Canary Islands, Spain, 2017, p. 38, https://doi.org/10.1117/12.2304098, nov.
[5] M. Bougoin, F. Mallet, J. Lavenac, A. Gerbert Gaillard, D. Ballhause, F. Chaumeil, «Full-SiC EUCLID's very large telescope», in: International Conference on Space Optics — ICSO 2018, Chania, Greece, 2019, p. 60, https://doi.org/10.1117/12.2535980, jul.
[6] D. Castel, E. Sein, S. Lopez, T. Nakagawa, y M. Bougoin, «The 3.2m All SiC Telescope for SPICA», Amsterdam, Netherlands, sep., 2012, p. 84502P, https://doi.org/10.1117/12.926891.
[7] S. Meyers, «Additive Manufacturing of Technical Ceramics», p. 178.
[8] «Very High Pressure Hot Pressing of Silicon Carbide», ResearchGate. https://www.researchgate.net/publication/279905556_Very_High_Pressure_Hot_Pressing_of_Silicon_Carbide (accedido abr. 15, 2019).
[9] Z.-Y. Hu, «A review of multi-physical fields induced phenomena and effects in spark plasma sintering: fundamentals and applications», Mater. Des. (2020) 54.
[10] R. Chaim, R. Marder, C. Estournés, Z. Shen, «Densification and preservation of ceramic nanocrystalline character by spark plasma sintering», Adv. Appl. Ceram. 111 (5-6) (2012) 280–285, https://doi.org/10.1179/1743676111Y.0000000074, ago.
[11] C. Manière, E. Nigito, L. Durand, A. Weibel, Y. Beynet, C. Estournès, «Spark plasma sintering and complex shapes: the deformed interfaces approach», Powder Technol. 320 (October) (2017) 340–345, https://doi.org/10.1016/j.powtec.2017.07.048.
[12] S. Prochazka, R.M. Scanlan, «Effect of boron and carbon on sintering of SIC», J. Am. Ceram. Soc. 58 (1-2) (1975) 72, https://doi.org/10.1111/j.1151-2916.1975.tb18990.x, ene.
[13] L. Stobierski, A. Gubernat, «Sintering of silicon carbideI. Effect of carbon», Ceram. Int. 29 (3) (2003) 287–292, https://doi.org/10.1016/S0272-8842(02)00117-7.
[14] L. Stobierski, A. Gubernat, «Sintering of silicon carbide II. Effect of boron», Ceram. Int. 29 (4) (2003) 355–361, https://doi.org/10.1016/S0272-8842(02)00144-X, ene.
[15] A. Maître, A.V. Put, J.P. Laval, S. Valette, G. Trolliard, «Role of boron on the spark plasma sintering of an α-SiC powder», J. Eur. Ceram. Soc. 28 (9) (2008) 1881–1890, https://doi.org/10.1016/j.jeurceramsoc.2008.01.002, ene.
[16] F. Guillard, A. Allemand, J.-D. Lulewicz, J. Galy, «Densification of SiC by SPS-effects of time, temperature and pressure», J. Eur. Ceram. Soc. 27 (7) (2007) 2725–2728, https://doi.org/10.1016/j.jeurceramsoc.2006.10.005, ene.
[17] S. Hayun, et al., «Microstructure and mechanical properties of silicon carbide processed by Spark Plasma Sintering (SPS)», Ceram. Int. 38 (8) (2012) 6335–6340, https://doi.org/10.1016/j.ceramint.2012.05.003, dic.
[18] E. Bernardo, I. Ponsot, P. Colombo, S. Grasso, H. Porwal, M.J. Reece, «Polymer-derived SiC ceramics from polycarbosilane/boron mixtures densified by SPS», Ceram. Int. 40 (9) (2014) 14493–14500, https://doi.org/10.1016/j.ceramint.2014.07.008, nov.
[19] Markusweinmann. Fritzaldinger, «Precursor-Derived Ceramics», p. 103.
[20] G.D. Soraru, F. Babonneau, J.D. Mackenzie, «Structural evolutions from polycarbosilane to SiC ceramic», J. Mater. Sci. 25 (September (9)) (1990) 3886–3893, https://doi.org/10.1007/BF00582455.
[21] M. Lodhe, N. Chawake, D. Yadav, M. Balasubramanian, «On correlation between β→α transformation and densification mechanisms in SiC during spark plasma sintering», Scr. Mater. 115 (2016) 137–140, https://doi.org/10.1016/j.scriptamat.2016.01.002, abr.
[22] Y. Lee, et al., «Phase transformation on spark plasma sintered dense polycarbosilane-derived SiC without additive», Scr. Mater. 143 (2018) 188–190, https://doi.org/10.1016/j.scriptamat.2017.02.031, ene.
[23] G. Boisselier, F. Maury, F. Schuster, «SiC coatings grown by liquid injection chemical vapor deposition using single source metal-organic precursors», Surf. Coat. Technol. 215 (2013) 152–160, https://doi.org/10.1016/j.surfcoat.2012.10.070, ene.
[24] L. Hongchao, K. Changlin, «Quantitative analysis of SiC polytype distributions by the rietveld method», J. Mater. Sci. 32 (May (10)) (1997) 2661–2664, https://doi.org/10.1023/A:1018623122324.
[25] L. Dobrzhinetskaya, et al., «Moissanite (SiC) with metal-silicide and silicon inclusions from tuff of Israel: Raman spectroscopy and electron microscope studies», Lithos 310-311 (June) (2018) 355–368, https://doi.org/10.1016/j.lithos.2017.04.001.
[26] S. Lafon-Placette, K. Delbé, J. Denape, M. Ferrato, «Tribological characterization of silicon carbide and carbon materials», J. Eur. Ceram. Soc. 35 (4) (2015) 1147–1159, https://doi.org/10.1016/j.jeurceramsoc.2014.10.038, abr.
[27] E. Lidén, L. Bergström, M. Persson, R. Carlsson, «Surface modification and dispersion of silicon nitride and silicon carbide powders», J. Eur. Ceram. Soc. 7 (6) (1991) 361–368, https://doi.org/10.1016/0955-2219(91)90059-9, ene.
[28] Y. Luo, M.Z. Rong, M.Q. Zhang, K. Friedrich, «Surface grafting onto SiC nanoparticles with glycidyl methacrylate in emulsion», J. Polym. Sci. Part Polym. Chem. 42 (15) (2004) 3842–3852, https://doi.org/10.1002/pola.20227, ago.
[29] W.M.M. Kessels, D.C. Marra, M.C.M. van de Sanden, E.S. Aydil, «*In situ* probing of surface hydrides on hydrogenated amorphous silicon using attenuated total reflection infrared spectroscopy», J. Vac. Sci. Technol. Vac. Surf. Films 20 (May (3)) (2002) 781–789, https://doi.org/10.1116/1.1469012.
[30] M.-W. Tsao, et al., «Studies of the solid-state conformation of polysilaethylene: an Organic/Inorganic hybrid polymer with an alternating C/Si backbone», Macromolecules 29 (22) (1996) 7130–7135, https://doi.org/10.1021/ma960267b, ene.
[31] W. J. Moberlychan, J. J. Cao, and L. C. D. Jonghe, «THE ROLES OF AMORPHOUS GRAIN BOUNDARIES AND THE b±a TRANSFORMATION IN TOUGHENING SiC», p. 11.
[32] E.Y. Tupitsyn, A. Arulchakkaravarthi, R.V. Drachev, T.S. Sudarshan, «Controllable 6H-SiC to 4H-SiC polytype transformation during PVT growth», J. Cryst. Growth 299 (February (1)) (2007) 70–76, https://doi.org/10.1016/j.jcrysgro.2006.10.258.

[33] E.A. Olevsky, L. Froyen, «Impact of thermal diffusion on densification during SPS», J. Am. Ceram. Soc. 92 (2009) S122–S132, https://doi.org/10.1111/j.1551-2916.2008.02705.x, ene.
[34] S.I. Cha, S.H. Hong, B.K. Kim, «Spark plasma sintering behavior of nanocrystalline WCÁ/10Co cemented carbide powders», Mater. Sci. Eng. A (2003) 8.
[35] C. Manière, L. Durand, G. Chevallier, C. Estournès, «A spark plasma sintering densification modeling approach: from polymer, metals to ceramics», J. Mater. Sci. 53 (May (10)) (2018) 7869–7876, https://doi.org/10.1007/s10853-018-2096-8.
[36] D.I. Yushin, A.V. Smirnov, N.W. Solis Pinargote, P.Y. Peretyagin, R. Torrecillas San Millan, «Modeling process of spark plasma sintering of powder materials by finite element method», Mater. Sci. Forum 834 (November) (2015) 41–50, https://doi.org/10.4028/www.scientific.net/MSF.834.41.